Structure, Physical Properties and Phase Transition of a Quasi-One-Dimensional Organic Semiconductor DBA(TCNQ)$_2$

Hailin Peng,[†] Chunbo Ran,[†] Zhongfan Liu,*[,†] Yunze Long,[‡] Zheming Wang,[§] Zhengqiang Yu,[§] Haoling Sun,[§] Yongge Wei,[§] Song Gao,[§] Zhaojia Chen,[‡] and Er-Qiang Chen[§]

Center for Nanoscale Science and Technology (CNST), Beijing National Laboratory for Molecular Sciences (BNLMS), State Key Laboratory for Structural Chemistry of Unstable and Stable Species, College of Chemistry and Molecular Engineering, Peking University, Beijing 100871, P. R. China, Key Laboratory of Extreme Conditions Physics, Institute of Physics, Chinese Academy of Sciences, Beijing 100080, P. R. China, and College of Chemistry and Molecular Engineering, Peking University, Beijing 100871, P. R. China

Received: March 5, 2008; Revised Manuscript Received: April 28, 2008

The present article investigates a reversible structural phase transition, and related physical properties change in a new quasi-one-dimensional (1D) organic semiconductor crystal, DBA(TCNQ)$_2$ [DBA = dibutylammonium, TCNQ = 7,7,8,8-tetracyanoquinodimethane]. Differential scanning calorimetry traces reveal the DBA(TCNQ)$_2$ single crystal undergoes a first-order reversible phase transition at around 260−270 K, which is accompanied by a dramatic change in both conductivity and magnetic susceptibility. A direct correlation of physical properties with crystal structure is established. Detailed X-ray structure analyses indicate a reversible structural change related to dimer−tetramer transition along the TCNQ chain and disruption of the hydrogen-bonding chains as the temperature decreases from 270 to 253 K, which is the origin of the electronic and magnetic transition.

1. Introduction

Organic charge-transfer (CT) complexes have been the subject of extensive investigations for the last four decades, beginning with the first reports of conducting salts of the powerful electron acceptor, 7,7,8,8-tetracyanoquinodimethane (TCNQ).[1,2] Planar TCNQ molecules are stacked face-to-face to form a quasi one-dimensional (1D) conductive chain structures in the CT complexes, which results in interesting electronic, optical, and magnetic properties.[3–5] The characteristic 1D molecular stacking arrangement plays a crucial role in their physical properties, such as spin/Peierls transitions, Mott−Hubbard transitions, and superconductivity. Recently, multifunctional CT materials exhibiting conducting properties as well as electric switching of two (or more) stable/metastable states using different external stimuli, such as an electric field,[6] current injection,[7,8] temperature,[9] pressure,[10] and so on, have received considerable attention because of their promising applications in organic light-emitting diode device and ultrahigh density memory. For example, the CT complex films of metals with TCNQ, such as Cu-TCNQ and Ag-TCNQ, are well-known to demonstrate electrically bistable switching and memory effects by applying an electric field or optical excitation.[11–15] In our recent work, a new quasi-one-dimensional CT complex semiconductor, DBA(TCNQ)$_2$ [DBA = dibutylammonium], was synthesized as a memory material,[16,17] and showed a *thermochemical hole burning* (THB) effect for ultrahigh density storage.[16–22]

In this paper, we focus our attention on the structural phase transition, and related physical properties change of the single crystal of DBA(TCNQ)$_2$. We report a first-order reversible phase change occurs at ca. 260−270 K, indicated by differential scanning calorimetry (DSC) traces. The phase transition is accompanied by a steep change in both conductivity and magnetic susceptibility. The temperature-dependent conductivity measurements exhibit an unusually inverted Peierls-like transition near 267 K on cooling and 270 K on heating, whereas the low-temperature semiconducting phase shows an increase in conductivity.[23] The temperature dependence of magnetic susceptibility clearly reveals a magnetic phase transition near 270 K on heating. To correlate the structural transition and the physical properties for quasi-one-dimensional electron system, we determine X-ray crystal structures at 270, 253, 240, and 290 K, respectively, which reveal the reversible structural change related to dimer-tetramer transition along the 1D TCNQ stacks and disruption of the hydrogen-bonding chains as the temperature decreases from 270 to 253 K.

2. Experimental Section

Preparation. A single crystal of DBA(TCNQ)$_2$ was synthesized from dibutylammonium iodide and TCNQ according to the method described previously,[16] typically exhibiting a needle shape with the size of several centimeters long, millimeters wide, and thick.

DSC Measurements. The DSC measurements for single crystals were performed on a Seiko Instruments EXSTAR 6000 model DSC6200 instruments. A scan was done by first cooling the sample to 233 K in dry nitrogen atmosphere and then taking the data while heating to 314 at 10 K min^{-1}. This was followed by a cooling scan to 233 at 10 K min^{-1}. A second heating and cooling scans in the 233−314 K range with a 10 K min^{-1} rate was carried out and produced similar data.

Electrical Transport Measurements. The standard four-probe method was used to measure the conductivity of the crystal along the length (*a*-axis) and two-probe method for the conductivities along the width and thickness (*b*- and *c*-axes),

* To whom correspondence should be addressed. Tel & Fax: 00-86-10-6275-7157. E-mail: zfliu@pku.edu.cn.

† Center for Nanoscale Science and Technology (CNST), Beijing National Laboratory for Molecular Sciences (BNLMS), State Key Laboratory for Structural Chemistry of Unstable and Stable Species, College of Chemistry and Molecular Engineering, Peking University.

‡ Chinese Academy of Sciences.

§ College of Chemistry and Molecular Engineering, Peking University.

10.1021/jp801928y CCC: $40.75
Published on Web 06/28/2008

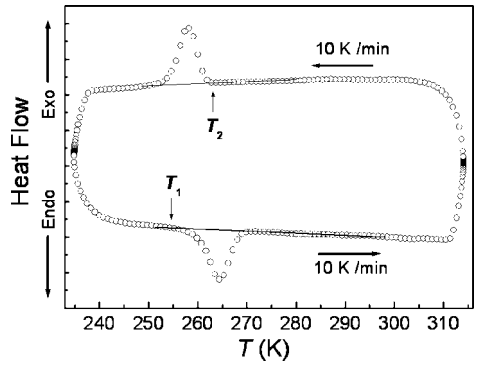

Figure 1. DSC traces of $DBA(TCNQ)_2$ with scanning rate of ± 10 K min^{-1}.

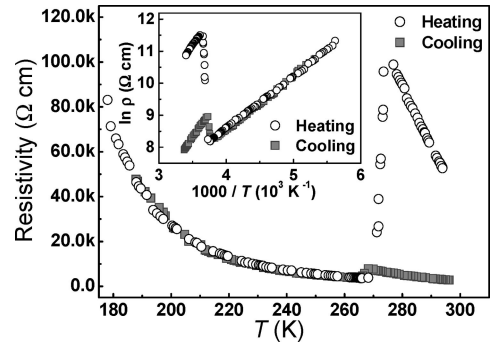

Figure 2. Temperature dependence of the resistivity for $DBA(TCNQ)_2$ along the *a*-axis on cooling and heating. Inset shows the plot of $\ln\rho$ versus $1000/T$.

respectively, using a Keithley 220-programmable current source and 181-nanovoltmeter, which were autocontrolled by a computer. For electrical contact, highly conductive silver paste was used. The data were collected by first cooling the sample from room temperature to the lowest temperature, followed by heating to room temperature, with a ca. 0.7 K min^{-1} rate.

Magnetic Measurements. The temperature dependence of the magnetic susceptibility was performed on a Quantum Design MPMS-XL7 SQUID. The sample was a set of random oriented needle-like single crystals with a total mass of 35.12 mg. Before a measuring field of 5.0 kOe was applied, the sample was zero-field-cooled to 2 K. The data set was taken while warming the sample from 2 to 300 K.

X-Ray Crystal Structure Analysis. A black crystal ($0.60 \times 0.45 \times 0.38$ mm^3) was selected for the single crystal X-ray diffraction analysis at different temperatures. The crystallographic data were first collected at 270 K on a Nonius Kappa CCD diffractometer with graphite-monochromated Mo/Kα radiation ($\lambda = 0.71073$ Å). The X-ray structure of the same crystal was subsequently determined at 253 and 240 K, respectively. Then the X-ray structure was determined at 290 K, after warming from 240 K and kept at 290 K for at least a day. The structures were solved by direct methods and refined by a full-matrix least-squares technique based on F^2 using the SHELXL 97 program. All non-hydrogen atoms were refined anisotropically, and hydrogen atoms were placed on the calculated positions and were refined isotropically. CCDC-261385 and 261386 contain the supplementary crystallographic data for this paper. These data can be obtained free of charge via www.ccdc.cam.ac.uk/conts/retrieving.html (or from the Cambridge Crystallographic Data Centre, 12, Union Road, Cambridge CB21EZ, UK; fax: (+44) 1223-336-033; or deposit@ccdc.cam.ac.uk).

3. Results and Discussion

3.1. DSC. To investigate the temperature-dependent physical properties of the $DBA(TCNQ)_2$ crystal, a DSC characterization was first used to determine phase transition temperature. Figure 1 represents the typical DSC traces in the 233−314 K range initiated with heating, followed by cooling, with a 10 K min^{-1} rate. The heating cycle clearly shows an endotherm with a peak near 264.4 K and the subsequent cooling scan has an exotherm with a peak near 258.2 K. A second heating and cooling scan in the same temperature range with the same rate produced similar data. These results indicate that the $DBA(TCNQ)_2$ crystal undergoes a first-order reversible phase transition. The transition showed some hysteresis (about 6 K), especially at faster heating/cooling rates (>20 K min^{-1}). The values of the transition temperatures corresponding to the observed thermal anomalies/peaks referred to the onset of the DSC peaks in the heating and cooling cycles, and those are 254 K (T_1) and 263 K (T_2), respectively. The change in enthalpy (ΔH) values associated with these thermal anomalies were obtained by averaging several measurements. The calculated ΔH values are 2.48 and −2.52 kJ mol^{-1} in the heating and cooling cycles, respectively.

3.2. Temperature-Dependent Conductivity. The room-temperature conductivities (σ) of a $DBA(TCNQ)_2$ crystal with a needle shape along three major crystal axes was found to be: $\sigma_a = 3.6 \times 10^{-4}$ S·cm^{-1}, $\sigma_b = 3.1 \times 10^{-6}$ S·cm^{-1}, and $\sigma_c = 1.8 \times 10^{-5}$ S·cm^{-1},[16] demonstrating a quasi-one-dimensional electronic nature. Extensive high-resolution scanning tunneling microscopy studies indicate that the TCNQ chains are along the *a*-axis (see the Supporting Information). We herein present further studies of temperature-dependent conductivity in detail.

Along three crystal axes, the temperature (T) dependences of resistivity (ρ) behave similarly (see the Supporting Information). Figure 2 shows a plot of T dependence of ρ along the *a*-axis in the range of 180−296 K. ρ increases gradually upon lowering T from 296 to 267 K, which reveals a semiconductive behavior with a gap energy (E_g) of 0.526 eV. A jump in resistivity by a factor of 1.8 occurs at about 267 K on cooling, suggesting a phase transition. Further cooling from 261 to 180 K shows again a semiconductive behavior, with $E_g = 0.286$ eV. The subsequent heating also reveals a semiconductive behavior with practically the same ρ and E_g as that associated with the cooling. A dramatic change of ρ by a factor of 23.4 occurs at 272 K on heating. The observation of hysteresis (5 K) suggests a first-order phase transition around 270 K, consistent with DSC measurement results. It is interesting that the high temperature phase on heating had a remarkably high resistivity but with the same E_g as seen on cooling (Figure 2 inset).

3.3. Magnetic Susceptibility. A plot of T dependence of χ_M and $\chi_M T$ for $DBA(TCNQ)_2$ in a field of 5 kOe in the temperature range of 2−300 K is shown in Figure 3, where χ_M is the molar magnetic susceptibility. The $\chi_M T$ value in the 2−20 K range was ca. 0.0047 cm^3 mol^{-1} K, which increases gradually with an increase of temperature from 20 to 270 K. On further heating, $\chi_M T$ increases abruptly from 270 to 274 K and then remains approximately constant from 274 to 300 K. The observed $\chi_M T$ value at 300 K is ca. 0.348 cm^3 mol^{-1} K. Note that χT still remains approximately constant from 300 to 400 K, suggesting no noticeable phase transition was observed above 300 K (see the Supporting Information). At temperatures lower than 20 K, the χ_M data is dominated by a Curie-like tail, presumably arising from magnetic defects, crystal imperfections, impurities, etc.[24]

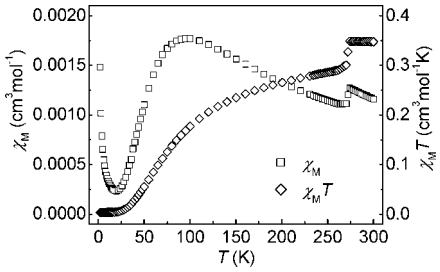

Figure 3. Plot of temperature dependence of the magnetic susceptibility χ_M and $\chi_M T$ for DBA(TCNQ)$_2$ measured at 5.0 kOe filed.

TABLE 1: Crystal Data and Structure Determination Details for DBA(TCNQ)$_2$ ($C_{32}H_{28}N_9$, M_r = 538.63, Triclinic, Space Group $P\bar{1}$, Z = 2) at 270 and 253 K

	270 K	253 K
a (Å)	6.6543(2)	13.172(3)
b (Å)	14.1920(4)	15.673(3)
c (Å)	15.9078(5)	7.8951(16)
α (deg)	83.3861(11)	90.40(3)
β (deg)	79.2127(11)	77.23(3)
γ (deg)	90.0183(15)	66.18(3)
vol (Å^{-3})	1465.56(8)	1445.8(5)
d_{calc} (g•cm^{-3})	1.221	1.237
F(000)	566	566
crystal size (mm^3)	0.60 × 0.45 × 0.38	
radiation, λ (Å)	Mo/Kα, 0.71073	
θ range (deg)	3.41−27.53	3.40−27.45
total no. of reflns measd	23541	23230
no. of unique reflns	6665	6560
R(int)	0.0555	0.0484
refinement method	full-matrix least-squares on F^2	
S, goodness-of-fit	0.948	0.967
final R indices	R_1 = 0.0634	R_1=0.0523
[$I > 2\sigma(I)$]	wR_2 = 0.1735	wR_2 = 0.1345
R indices (all data)	R_1 = 0.1486	R_1 = 0.1185
	wR_2 = 0.2092	wR_2 = 0.1591
max shifted/esd	0.001	0.001
min peak in diff Fourier map (e Å^{-3})	−0.260	−0.316
max peak in diff Fourier map (e Å^{-3})	0.354	0.441
max peak in diff Fourier map (e Å^{-3})		

3.4. Structural Change. To study the phase transition of DBA(TCNQ)$_2$, the X-ray crystal structure of DBA(TCNQ)$_2$ was determined at 270, 253, and 240 K successively. Then its structure was determined at 290 K when the same sample was warmed from 240 K and kept at ca. 290 K for at least a day. Parameters of crystallographic data collection and refinement for both 270 and 253 K are listed in Table 1. A structural change between 253 and 270 K is observed, and the structure determined at 240 K was strong analogous to that at 253 K. In addition, there is no substantial difference between the structures at 290 and 270 K, indicating the structural phase change is reversible.

Figure 4 depicts the molecular structure and the atomic numbering in the asymmetric unit of DBA(TCNQ)$_2$ at 270 K. Above the transition temperature, at 270 K, the DBA(TCNQ)$_2$ crystal is triclinic with space group $P\bar{1}$ and a = 6.6543, b = 14.192, and c = 15.908 Å; α = 83.39, β = 79.21, and γ = 90.02°; vol = 1465.6 Å^3; and Z = 2. A DBA cation and two crystallographically independent TCNQ molecules (A and B) exists in the asymmetric unit (Figure 5). The planar TCNQ molecules are stacked face-to-face with repeat sequence AB leading to two independent spacing distances (d_{AB} = 3.25 Å, $d_{BA'}$ = 3.39 Å). The packing can be described as a set of TCNQ columns (in effect, a stack of AB diads) parallel to the a direction and spaced by chains of DBA cations in the b direction. Both intra- and interdimer overlap modes are analogous and approached the ring-external-bond type. The separate TCNQ(B) molecules are linked together via two hydrogen (H-) bonds from adjacent DBA cations, so that two sheets of H-bonded TCNQ(B) and DBA are separated by a sheet of non H-bonded (isolated) TCNQ(A) molecules along the a direction (Figure 5). Table 2 shows the distances and angles of H-bonds at 270 K. The N···N distances between N9 of DBA and the two cyanide nitrogens N4 and N1 of separate molecules TCNQ(B) are 3.137(3) and 2.895(4) Å, respectively.

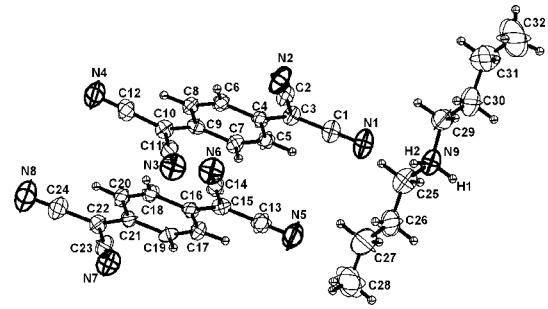

Figure 4. Asymmetric unit of the complex DBA(TCNQ)$_2$ showing the atomic numbering at 270 K. Thermal ellipsoids are drawn at the 50% probability level.

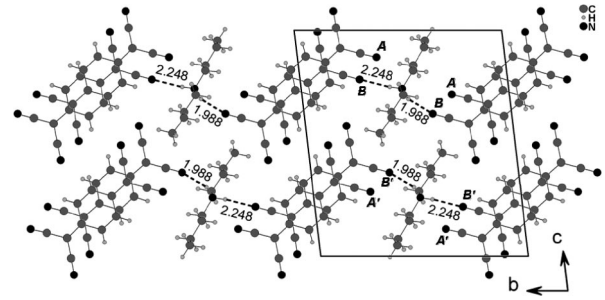

Figure 5. Crystal structure at 270 K viewed along the a-axis. The dashed lines indicate hydrogen bonds.

TABLE 2: Bond Distances (Å) and Angles (deg) to Hydrogen Bonds Related for DBA(TCNQ)$_2$ at 270 K

D−H···A	d(D−H)	d(H···A)	d(D···A)	(D−H···A)
N9−H1···N4^a	0.89(2)	2.25(2)	3.137(3)	173.8(22)
N9−H2···N1^b	1.03(3)	1.99(3)	2.895(4)	145.4(23)

^{a} Symmetry transformations used to generate equivalent atoms: x, $-1 + y$, z. ^{b} Symmetry transformations used to generate equivalent atoms: x, y, z.

Below the transition temperature, at 253 K, the crystal retains the same space group. The unit cell parameters are a = 13.172(3), b = 15.673(3), and c = 7.8951(16) Å; α = 90.40(3), and β = 77.23(3), γ = 66.18(3)°; vol = 1445.8(5) Å^3; and Z = 2. Thus, the unit cell is doubled along the a-direction but halved along the c-direction, as compared with that at 270 K. Figure 6 gives molecular structure and the atomic numbering in the asymmetric unit of DBA(TCNQ)$_2$ at 253 K. The TCNQ(A) and TCNQ(B) molecules stack as ABB′A′−ABB′A′ tetramer along the a-axis, leading to three independent spacing distances ($d_{AA'}$ = 3.49 Å, d_{AB} = 3.15 Å, $d_{BB'}$ = 3.34 Å) and three independent overlap modes (Figure 7). Figure 8 shows three overlap modes of adjacent TCNQ molecules that are of the "ring-external-bond" type with some deviations from the ideal position. The inter-tetramer overlap mode A′A shows larger transverse relative shift

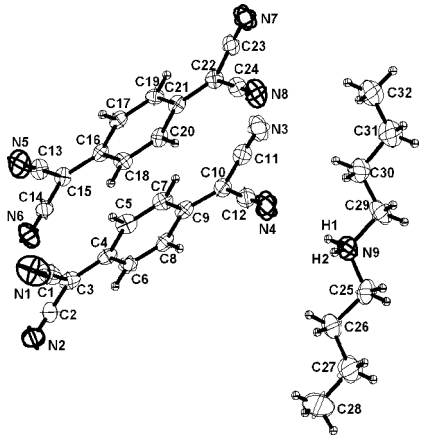

Figure 6. Asymmetric unit of the complex $DBA(TCNQ)_2$ showing the atomic numbering at 253 K. Thermal ellipsoids are drawn at the 50% probability level.

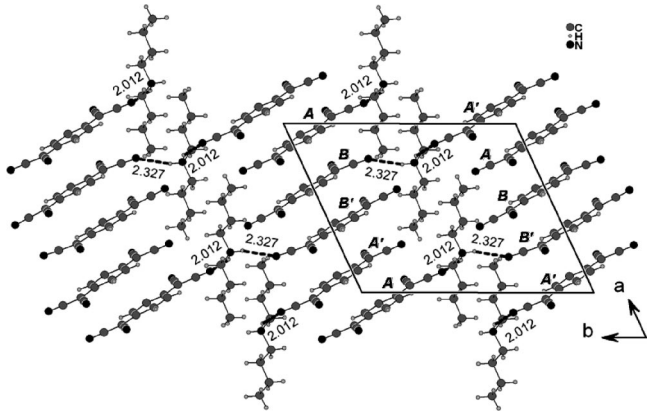

Figure 7. Crystal structure at 253 K viewed along the *c*-axis. The dashed lines indicate hydrogen bonds.

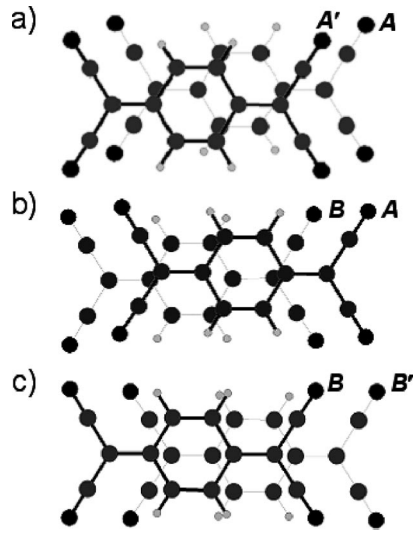

Figure 8. Projection of two neighboring TCNQ molecules in $DBA(TCNQ)_2$ along the normal to the *p*-quinodimethane least-squares plane at 253 K: (a) molecules A′ and A, (b) molecules A and B, (c) molecules B and B′.

of the TCNQ centroids than the other two types of overlap modes, AB and BB′, within the TCNQ tetramer.

It is worth noting that the H-bonding network changes during the phase change. H-bonds distances and angles between the DBA cation and TCNQ molecules at 253 K are listed in Table 3, and the corresponding atomic numbering are indicated in Figure 6. The N···N distances between N9 of DBA and the two cyanide nitrogens, N4 of TCNQ(B) and N8 of TCNQ(A), are 3.160(3) and 2.885(3) Å, respectively. As shown in Figure 7, every DBA cation is oriented in such a way to form two bifurcated H-bonds′ bridges with TCNQ(A) and TCNQ(B) in the separate stacks. Every TCNQ molecule only links one H-bond with the adjacent DBA. Thus, one end of every TCNQ is perturbed via C≡N···H interactions, whereas the other ends are free. Consequently, below the transition temperature, the H-bonding chains occurring in the sheets of H-bonded TCNQ(B) and DBA in the high temperature phase are disrupted.

TABLE 3: Bond Distances (Å) and Angles (deg) Related to Hydrogen Bonds for $DBA(TCNQ)_2$ at 253 K

D−H···A	*d*(D−H)	*d*(H···A)	*d*(D···A)	<(D−H···A)
N9−H1···N4[a]	0.87(2)	2.33(2)	3.160(3)	160.3(18)
N9−H2···N8[b]	0.98(2)	2.01(2)	2.885(3)	147.4(17)

[a] Symmetry transformations used to generate equivalent atoms: $-x+1, -y, -z+2$. [b] Symmetry transformations used to generate equivalent atoms: $x-1, y+1, z+1$.

TABLE 4: Mean Bond Lengths (Å) of the TCNQ Molecules in $DBA(TCNQ)_2$, Neutral $TCNQ^0$, and Fully Ionized $TCNQ^-$ in RbTCNQ

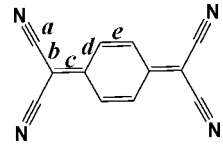

		a	*b*	*c*	*d*	*e*
$DBA(TCNQ)_2$						
270 K	TCNQ(A)	1.144	1.428	1.386	1.435	1.344
	TCNQ(B)	1.152	1.421	1.407	1.421	1.361
253 K	TCNQ(A)	1.146	1.420	1.398	1.430	1.354
	TCNQ(B)	1.149	1.422	1.398	1.428	1.357
$TCNQ^0$		1.140	1.441	1.374	1.448	1.346
$TCNQ^-$		1.153	1.416	1.420	1.423	1.373

It is important to evaluate the degree of charge transfer (δ) in the CT complexes, because the electric properties are sensitive to δ.[25,26] $DBA(TCNQ)_2$ is a radical-ion salt and thus the total degree of charge transfer (δ_t) between DBA cation and TCNQ anions is exactly 1 e except perhaps for hypothetical back transfer of electrons. The charge-transfer value can be estimated by the method suggested by Kistenmacher et al.,[27,28] from the well-known relationship $\delta = M[c/(b+d)] + N$ e ($M = 41.667$ and $N = -19.833$ are determined from neutral $TCNQ^0$ ($\delta =$ 0 e) and fully ionized $TCNQ^-$ in RbTCNQ ($\delta = 1$ e)).[28–31] The values of *c*, *b* and *d* are average bond lengths of TCNQ (listed in Table 4). At 270 K, the δ_A and δ_B representing the charge-transfer values for the TCNQ(A) and TCNQ(B) molecules, normalized to $\delta_t = 1$ e, were 0.27 and 0.73 e, respectively. Hence, at 270 K, the unit charge is mainly pinned on the specific TCNQ(B). However, both δ_A and δ_B are estimated as 0.5 e at 253 K, suggesting all TCNQ are equivalent in the TCNQ chain.

3.5. Correlation of Structural Transition and Physical Properties. The TCNQ-based CT complexes constitute a class of organic solids that are of special interest because of their quasi one-dimensional nature, reflected in their electronic and magnetic properties, as well as their phase transitions. Peierls first reported that a half-filled one-dimensional band will show a phase transition to a demerized phase,[23] and Beni and Pincus found that a similar chain transition will occur in an infinite one-dimensional chain of spins.[32] $DBA(TCNQ)_2$ is one of the model materials in quasi one-dimensional electron system. The

conductivities and other physical properties of $DBA(TCNQ)_2$ can be explained qualitatively by its characteristic 1D TCNQ stacking arrangements.

The $DBA(TCNQ)_2$ crystal undergoes reversible structural transition near 267 K, related to dimer-tetramer transition along the TCNQ chain and disruption of the hydrogen-bonding chains as the temperature is reduced from 270 to 253 K. The change in enthalpy (ΔH) values related to the thermal anomalies in the DSC traces was 2.48 kJ mol^{-1} and -2.52 KJ mol^{-1} in the heating and cooling cycles, respectively, consistent with the breakage and reformation of the H-bonds.

The structural transition accompanies a steep change in both conductivity and magnetic susceptibility. The temperature-dependent conductivity of $DBA(TCNQ)_2$ indicates a semiconductor-semiconductor transition around 267 K, characterized as a inverted Peierls-like transition behavior in which the lower temperature phase has a higher conductivity due to a lower activation energy for the electron hopping. The origin of the inverted Peierls-like transition can be discussed with the results of structural transition.

The conductivity for the complex salts of tertiary amines with TCNQ is largely determined by the connectivity of a conductive path, the array of charged TCNQ molecules, and the uniformity of the charge distribution in the TCNQ stacks.[30] The inverted Peierls-like transition behavior of $DBA(TCNQ)_2$ might be attributed to the change of the charge distribution in the TCNQ chains, which arises from the structural change related to dimer-tetramer transition along the TCNQ chain and the disruption of the H-bonding network within the crystal. Above T_c, at 270 K, the stacks contained TCNQ dimers with an intradimer distance of $d_{AB} = 3.25$ Å; successive dimers are separated by 3.39 Å. Below T_c, at 275 K, the intertetramer distance ($d_{AA'} = 3.49$ Å) is relatively large, and the intertetramer overlap mode A′A shows a relatively larger transverse shift than the overlap modes within the TCNQ tetramer. These features at 253 K may inhibit the connectivity of the array of charged TCNQ molecules to some extent. However, the remarkably small intradimer distance ($d_{AB} = 3.15$ Å) at 253 K gives rise to a strong π-orbital overlap between adjacent TCNQ(A) and TCNQ(B) molecules in the tetramer, which facilitates the connectivity of charged TCNQ molecules and the uniformity of the distribution of charge in the chains.

Below T_c, TCNQ were equivalent, arising from the effective overlap of adjacent TCNQ molecules and the H-bonds of DBA cation with both TCNQ(A) and TCNQ(B). In contrast, above T_c, a relatively large disparity exists in the ionicity ($\rho_A = 0.27$ e and $\rho_B = 0.73$ e at 270 K) of the TCNQ stacks. H-bonding links DBA cation with TCNQ(B). Thus, H-bonds result in the "pinning" of formal charge on special TCNQ(B), which may limit the charge mobility and, therefore, inhibit the electrical conductivity in the TCNQ chain.

As described previously, the resistivity of the high temperature phase on heating was remarkably higher than that observed on cooling, though they had the same E_g (see Figure 2 inset). This observation may be understood by considering stress induced defect in the TCNQ chains during the structural change: as the temperature increases from 253 to 270 K, TCNQ chains in $DBA(TCNQ)_2$ change from a tetramerization to a dimerization phase, the lattice constant along the *a*-axis expands by ~1%. Consequently, a stress presumably induces the defects or transient/metastable domains to form in the TCNQ chains, which inhibits the electrical conductivity of TCNQ chains and, therefore, gives rise to a dramatic drop in the conductance of crystal.

The magnetic susceptibility of $DBA(TCNQ)_2$ also suddenly change at ca. 270 K on heating, suggesting the electronic transition was coupled to the simultaneous magnetic transition. Below T_c, each TCNQ dimer possessed a localized spin of $^1/_2$ and successive dimers coupled antiferromagnetically, which may cause a sharp drop in the magnetic susceptibility. The magnetic susceptibility of $DBA(TCNQ)_2$ will be further explored by careful temperature-dependent specific-heat measurements and adequate spin models in the future.

4. Conclusion

We have investigated the X-ray crystal structure and the structural transition, electrical transport, magnetic properties of a new quasi-one-dimensional semiconductor crystal, $DBA(TCNQ)_2$. DSC traces reveal that the $DBA(TCNQ)_2$ crystal undergoes a first-order reversible phase transition at around 260−270 K, which is accompanied by a steep change in both conductivity and magnetic susceptibility, as a characteristic of an electronic and magnetic transition. Detailed X-ray structure analyses indicate a structural change related to dimer-tetramer transition along the TCNQ chain and disruption of the hydrogen-bonding chains as the temperature is reduced from 270 to 253 K, which is the origin of the electronic and magnetic transition.

Acknowledgment. H.P. thanks Yuan Li and Guichuan Yu at Stanford University for help with magnetic measurements. This work was supported by NSFC (90301006, 50521201) and MOST (2007CB936203, 2006CB932403, 2006CB932602).

Supporting Information Available: STM studies of $DBA(TCNQ)_2$, temperature-dependent resistivities of a $DBA(TCNQ)_2$ single crystal along three crystal axes, Magnetic measurements in the temperature range 10−400 K. This material is available free of charge via the Internet at http://pubs.acs.org.

References and Notes

(1) Acker, D. S.; Harder, R. J.; Hertler, W. R.; Mahler, W.; Melby, L. R.; Bensin, R. E.; Mochel, W. E. *J. Am. Chem. Soc.* **1960**, *82*, 6408.
(2) Melby, L. R.; Harder, R. J.; Hertler, W. R.; Mahler, W.; Benson, R. E.; Mochel, W. E. *J. Am. Chem. Soc.* **1962**, *84*, 3374.
(3) Xiao, K.; Ivanov, I. N.; Puretzky, A. A.; Liu, Z.; Geohegan, D. B. *Adv. Mater.* **2006**, *18*, 2184.
(4) Coronado, E.; Day, P. *Chem. Rev.* **2004**, *104*, 5419.
(5) Di, C.; Yu, G.; Liu, Y.; Xu, X.; Wei, D.; Song, Y.; Sun, Y.; Wang, Y.; Zhu, D.; Liu, J.; Liu, X.; Wu, D. *J. Am. Chem. Soc.* **2008**, *128*, 16418.
(6) Gao, H. J.; Sohlberg, K.; Xue, Z. Q.; Chen, H. Y.; Hou, S. M.; Ma, L. P.; Fang, X. W.; Pang, S. J.; Pennycook, S. J. *Phys. Rev. Lett.* **2000**, *84*, 1780.
(7) Kumai, R.; Okimoto, Y.; Tokura, Y. *Science* **1999**, *284*, 1645.
(8) Okimoto, Y.; Kumai, R.; Saitoh, E.; Izumi, M.; Horiuchi, S.; Tokura, Y. *Phys. Rev. B* **2004**, *70*, 115104.
(9) Laukhina, E.; Vidal-Gancedo, J.; Laukhin, V.; Veciana, J.; Chuev, I.; Tkacheva, V.; Wurst, K.; Rovira, C. *J. Am. Chem. Soc.* **2003**, *125*, 3948.
(10) Hutchison, K. A.; Srdanov, G.; Menon, R.; Gabriel, J. P.; Knight, B.; Wudl, F. *J. Am. Chem. Soc.* **1996**, *118*, 13081.
(11) Potember, R. S.; Poehler, T. O.; Benson, R. C. *Appl. Phys. Lett.* **1982**, *41*, 548.
(12) Potember, R. S.; Poehler, T. O.; Cowan, D. O. *Appl. Phys. Lett.* **1979**, *34*, 405.
(13) Gu, Z. Z.; Wu, H. M.; Wei, Y.; Liu, J. Z. *J. Phys. Chem.* **1993**, *97*, 2543.
(14) Oyamada, T.; Tanaka, H.; Matsushige, K.; Sasabe, H.; Adachi, C. *Appl. Phys. Lett.* **2003**, *83*, 1252.
(15) O'Mullane, A. P.; Neufeld, A. K.; Bond, A. M. *Anal. Chem.* **2005**, *77*, 5447.
(16) Peng, H. L.; Ran, C. B.; Yu, X. C.; Zhang, R.; Liu, Z. F. *Adv. Mater.* **2005**, *17*, 459.

(17) Yu, X. C.; Zhang, R.; Peng, H. L.; Ran, C.; Zhang, Y. Y.; Liu, Z. F. *J. Phys. Chem. B* **2004**, *108*, 14800.
(18) Peng, H. L.; Chen, Z.; Tong, L. M.; Yu, X. C.; Ran, C. B.; Liu, Z. F. *J. Phys. Chem. B* **2005**, *109*, 3526.
(19) Yu, X. C.; Peng, H. L.; Ran, C. B.; Sun, L.; Zhang, R.; Liu, Z. F. *Appl. Phys. Lett.* **2005**, *86*, 133105.
(20) Huang, X. M.; Lin, F.; Zhou, W.; Ren, L.; Peng, H. L.; Liu, Z. F. *J. Phys. Chem. C* **2008**, *112*, 2004.
(21) Ran, C. B.; Peng, H. L.; Ren, L.; Zhou, W.; Ling, Y. D.; Liu, Z. F. *J. Phys. Chem. C* **2007**, *111*, 631.
(22) Ran, C. B.; Peng, H. L.; Zhou, W.; Yu, X. C.; Liu, Z. F. *J. Phys. Chem. B* **2005**, *109*, 22486.
(23) Peierls, R. E. *Quantum Theory of Solids*; Oxford University: London, 1955.
(24) Liu, H.-L.; Chou, L. K.; Abboud, K. A.; Ward, B. H.; Fanucci, G. E.; Granroth, G. E.; Canadell, E.; Meisel, M. W.; Talham, D. R.; Tanner, D. B. *Chem. Mater.* **1997**, *9*, 1865.
(25) Torrance, J. B.; Scott, B. A.; Kaufman, F. B. *Solid State Commun.* **1975**, *17*, 1369.
(26) Torrance, J. B.; Mayerle, J. J.; Bechgaard, K.; Silverman, B. D.; Tomkiewicz, Y. *Phys. Rev. B* **1980**, *22*, 4960.
(27) Kistenmacher, T. J.; Emge, T. J.; Blcoch, A. N.; Cowan, D. O. *Acta Crystallogr. B* **1982**, *38*, 1193.
(28) Miyasaka, H.; Campos-Fernández, C. S.; Clérac, R.; Dunbar, K. R. *Angrew. Chem.* **2000**, *112*, 3989.
(29) Long, R. E.; Sparks, R. A.; Trueblood, K. N. *Acta Crystallogr.* **1965**, *18*, 932.
(30) Hoekstra, A.; Spoelder, T.; Vos, A. *Acta Crystallogr. B* **1972**, *28*, 14.
(31) Bandrauk, A. D.; Ishii, K.; Truong, K. D.; Aubin, M.; Hanson, A. W. *J. Phys. Chem.* **1985**, *89*, 1478.
(32) Beni, G.; Pincus, P. *J. Chem. Phys.* **1972**, *57*, 3531.

JP801928Y